Insights into Imaging

**ESR** EUROPEAN SOCIETY OF RADIOLOGY

**CRITICAL REVIEW**

**Open Access**

# Methodological considerations on segmenting rhabdomyosarcoma with diffusion-weighted imaging—What can we do better?

Cyrano Chatziantoniou[1,2]* , Reineke A. Schoot[2], Roelof van Ewijk[2], Rick R. van Rijn[4], Simone A. J. ter Horst[2,5], Johannes H. M. Merks[2], Alexander Leemans[1] and Alberto De Luca[1,3]

## Abstract

**Purpose**  Diffusion-weighted MRI is a promising technique to monitor response to treatment in pediatric rhabdomyosarcoma. However, its validation in clinical practice remains challenging. This study aims to investigate how the tumor segmentation strategy can affect the apparent diffusion coefficient (ADC) measured in pediatric rhabdomyosarcoma.

**Materials and methods**  A literature review was performed in PubMed using search terms relating to MRI and sarcomas to identify commonly applied segmentation strategies. Seventy-six articles were included, and their presented segmentation methods were evaluated. Commonly reported segmentation strategies were then evaluated on diffusion-weighted imaging of five pediatric rhabdomyosarcoma patients to assess their impact on ADC.

**Results**  We found that studies applied different segmentation strategies to define the shape of the region of interest (ROI)(outline 60%, circular ROI 27%), to define the segmentation volume (2D 44%, multislice 9%, 3D 21%), and to define the segmentation area (excludes edge 7%, excludes other region 19%, specific area 27%, whole tumor 48%). In addition, details of the segmentation strategy are often unreported. When implementing and comparing these strategies on in-house data, we found that excluding necrotic, cystic, and hemorrhagic areas from segmentations resulted in on average 5.6% lower mean ADC. Additionally, the slice location used in 2D segmentation methods could affect ADC by as much as 66%.

**Conclusion**  Diffusion-weighted MRI studies in pediatric sarcoma currently employ a variety of segmentation methods. Our study shows that different segmentation strategies can result in vastly different ADC measurements, highlighting the importance to further investigate and standardize segmentation.

### Key points

- Strategies for segmenting sarcoma tumors vary widely throughout literature.
- Details of the segmentation strategy are often not reported.
- Including necrotic or cystic areas in the segmentation affects diffusion measurements.

*Correspondence:
Cyrano Chatziantoniou
c.chatziantoniou-3@umcutrecht.nl
Full list of author information is available at the end of the article

Springer Open

Chatziantoniou *et al. Insights into Imaging*     (2023) 14:19

Page 2 of 15

- Varying the slice of a single-slice segmentation can drastically impact diffusion measurements.

**Keywords**  Sarcoma, Magnetic resonance imaging, Rhabdomyosarcoma

## Introduction

Rhabdomyosarcoma is an aggressive tumor that can arise in any part of the body and is thought to stem from primitive mesenchymal cells. Rhabdomyosarcoma is the most common soft tissue sarcoma in children and adolescents and requires multimodal treatment including chemotherapy and local therapy (surgery and/or radiotherapy). Although therapy advances have been made over het last decades, important improvements in therapy are needed as patients with high risk disease have suboptimal survival. Markers of response for pediatric rhabdomyosarcoma are urgently needed for the evaluation of new agents in clinical trials, and to support (de) intensification of treatment for individual patients. Since rhabdomyosarcoma is a rare disease (with an incidence of about 4.5 cases per million children [1]), collaborative, international multicenter studies are necessary to achieve a sample size that is sufficient to identify and validate biomarkers. To date, the change in tumor size is used to evaluate response and to support decisions to continue or change (systemic) treatment. However, in the past decade, several studies have challenged the prognostic value of change in size in relation to outcome [2–7]. Additionally, size response has been criticized for its moderate reproducibility between observers [8]. Therefore, there is a clear need for a new early response biomarker that can impact prognosis. It has been suggested that diffusion-weighted MRI (DWI)-based radiomics may provide such a prognostic marker.

Previous exploratory studies have suggested the existence of a relation between water diffusion in the tumor and tumor response [9, 10]. The general theory behind this relation is that a decrease in tumor cellularity due to therapy increases the rate of water diffusion, leading to a higher quantified diffusion-weighted MRI parameter, the apparent diffusion coefficient (ADC) [11, 12]. Similar studies have examined this relation for other tumors, with mixed results [11, 13, 14]. To date, no study has reliably demonstrated whether ADC could predict response to treatment in rhabdomyosarcoma with sufficient accuracy [9].

An important aspect of DWI-based radiomics is the definition of the region of interest (ROI) used to measure the ADC. To date there are no international guidelines describing how these regions should be defined, and as such different strategies are being used [5]. Although apparently straightforward, a segmentation strategy consists of many methodological choices and parameters. These include, for example, the number of slices included in the analysis, whether to draw a polygonal outline following the tumor border or a circular ROI, and which part(s) of the tumor to include. Currently, despite the ubiquitous use of segmentations to measure the ADC in tumors, little is known on how these choices affect the ADC measurements.

To address this knowledge gap, we explored how segmentation strategies differ in recent studies relating to sarcomas. To this end, we first performed a literature review to gather which methods are most commonly applied for tumor segmentation in sarcoma imaging. Second, we conducted a pilot study to investigate the impact of the choice of a selected number of segmentation strategies on the ADC measured in pediatric rhabdomyosarcoma.

## Methods

Our study consists of two main parts. In the first part, we performed a literature review on tumor segmentation methods applied in sarcoma research. In the second part, we explored the impact of the choice of a number of segmentation strategies on the ADC measured in a representative sample of pediatric rhabdomyosarcoma cases.

### Literature review
#### Literature search
A literature search was performed using PubMed on 24-03-2022. The search included terms on MRI and sarcomas (see Additional file 1). Publication language was restricted to English. Publication status was not restricted. Articles were excluded if they did not mention or imply MRI and segmentation of sarcomas in the title or abstract. Based on the full text, articles were furthermore excluded if DWI was not performed, if no details on segmentation methods were present, or if MRI was only done on animal models. Additionally, given the focus of this work on sarcomas, articles were excluded if they reported on less than 10 sarcoma patients and if those patients constituted less than 50% of the total patient population. An overview of the selection is shown in Fig. 1.

#### Segmentation strategy details
For the remaining 76 articles, details on the segmentation of the tumors were collected. Two papers used
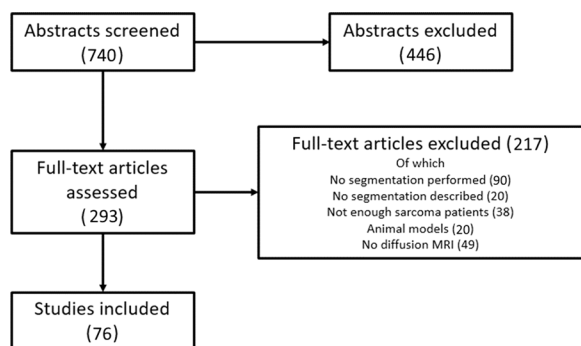
**Fig. 1** From the 740 studies in the search, 446 were excluded based on the title or abstract. Articles were excluded if they did not mention or imply MRI and segmentation of a sarcoma. Next, out of the 293 remaining articles, 217 were excluded based on the full text. Articles were excluded if no DWI was performed, if no details on segmentation were present, or if MRI was only performed on animals. Additionally, articles were excluded if they included less than 10 sarcoma patients and those patients constituted less than 50% of the total patient population

multiple methods. These have all been included as separate strategies.

The details of interest were the image modality (diffusion, structural), the segmentation method (outline, circular ROI), the segmentation area (whole tumor, excludes edge, excludes other, specific area), and the segmentation volume (2D, multislice, 3D). Here, we define a multislice segmentation as a segmentation on multiple, but not all, slices where a tumor is present. Whenever a paper did not explicitly state the individual aspects and did not provide any other information from which they could be determined, that aspect was noted as 'unclear.' Some articles excluded both the edge and other areas. These were then both counted. We lastly recorded whether any aspects of the segmentation strategies were justified with a reference to another study.

### Segmentation analysis

In order to quantitatively compare the effects of different segmentation strategies on ADC measurements, we selected six segmentation methods that best represented the majority of the strategies found in the literature review (for details, see literature review results). They were then used to segment DWI images of pediatric rhabdomyosarcoma patients. In order to gain some insight into how the ADC distribution might vary throughout the tumor, as well as to gauge the robustness of single-slice segmentations,

these segmentations were applied on a slice nearby the initial one.

### Patients

Five pediatric rhabdomyosarcoma patients were selected from a cohort treated at Princess Máxima Center (Utrecht, the Netherlands). Explicit consent was obtained for all patients. Patients were selected to represent different tumor sizes, as well as different amounts of necrotic and cystic areas present. Patients were all male, 1–17 years of age, with either an embryonal (n = 3, fusion negative), alveolar (n = 1, PAX7-FOXO1 positive), or sclerosing rhabdomyosarcoma (n = 1). Three primary tumors were located in the bladder, one in the lower extremity and one in the upper extremity. Patients were all treated and imaged according to the E*p*SSG RMS 2005 protocol [15]. Only imaging performed at diagnosis (i.e., before treatment) was used for this analysis.

### Image analysis

Image segmentation was performed by two pediatric radiologists (S.H. and R.R.) with 10 and 18 years of experience in pediatric oncology. All segmentations were subsequently reviewed in a consensus reading with both radiologists. Prior to segmenting, the slice with the largest cross-sectional tumor area was manually identified.

The regions of interest were annotated via an in-house developed program that allowed the radiologists to place a polygon on the outline of the tumors and circles within the tumor. The polygon's edges could be moved after initial placement to refine the segmentation when needed. The segmentation was performed on ADC maps, and raters could refer to corresponding T1, T1 + Gadolinium, or T2 images during the process for additional information.

For each patient, six ROIs were drawn. These were based on the most frequently occurring strategies identified in our review. The ROIs were drawn on the axial slice with the largest tumor area. The raters first drew the whole outline and then repeated the outline slightly (2 mm) inside the outer edge. Next, they drew an additional outline along the edges of any necrotic, cystic, or hemorrhagic components. Any solid areas within these components were included in this outline. Lastly, they drew the large circular ROI as well as the smaller circular ROIs. The small circular ROIs were placed in three areas with a high degree of diffusion restriction, which was identified visually by the radiologists based on the ADC images. Segmentations could be hidden in the program to allow the raters to draw multiple ROIs on a single slice

without it becoming too cluttered. Another set of six ROIs was then drawn in the exact same manner on a slice two steps down in the caudal direction.

### Statistical analysis

To evaluate whether different segmentation methods lead to different ADC distributions within the ROIs, a two-sample Kolmogorov–Smirnov test was performed between the results of any pair of methods. This test was chosen based on its ability to pairwise compare distributions without making prior assumptions on their shape.

Another two-sample Kolmogorov–Smirnov test was applied to ADC values measured on different slices for all strategies. This was done to determine whether the choice of slice used in a single-slice annotation might lead to a difference in ADC distribution.

## Results

### Literature review

The literature search yielded 740 results. From these, 446 were excluded based on the title or abstract. Out of the 293 remaining articles, 217 were excluded based on the full text. Twenty articles were excluded based on full text due to unclear reporting; they did not report any details at all on the segmentation strategy, while segmentation was implied or stated to be performed. In total 76 articles were included. An overview of the included papers is shown in Fig. 1. Details on the included articles are listed in Table 1. The patients included in the 76 articles were: rhabdomyosarcoma 6.6% (5 articles), out of which 5.3% (4 articles) pediatric rhabdomyosarcoma; osteosarcoma 21.1% (16 articles); uterine sarcoma 11.8% (9 articles); hepatic angiosarcoma 1.3% (1 article); leiomyosarcoma 6.6% (5 articles); endometrial stromal sarcoma 1.3% (1 article); pulmonary artery sarcoma 1.3% (1 article); chondrosarcoma 3.3% (2 articles); and multiple soft tissue sarcomas 47.4% (36 articles).

An overview of the different aspects of each segmentation strategy and its usage is shown in Table 2. For the segmentation method, drawing an outline was most common (49), compared to placing a circular ROI (22). Most studies performed single-slice segmentations (36), followed by segmentations on all slices (17) and multislice segmentation (7). Virtually all segmentations were performed manually (79) with only two strategies being semi-automated. Most segmentations were done on DWI data (70), with six strategies segmenting on structural images (T1/T2) and transferring to DWI data afterward. Most strategies segmented the whole tumor (39), or a specific area (22). Some strategies excluded necrotic, cystic, or hemorrhagic areas (15), and a few studies

excluded the peripheral areas of the tumor (6). Some studies placed multiple, usually circular, ROIs (7).

Table 2 additionally shows that a number of studies do not report all aspects of the employed segmentation strategy. We found the following frequencies of unreported details of the segmentation strategies: zero (55 studies), one (19 studies), two (4 studies), three or more (3 studies). The majority of included studies report all aspects we intended to analyze, 54/81. Nineteen studies did not mention one aspect and eight studies failed to report two or more aspects.

Out of the 76 articles, eight included one or more references to other works regarding segmentation strategies. These references provided background on the inclusion or exclusion of a region for segmentation (seven articles) and the definition of a region to be segmented (four articles).

Based on these results, six segmentation approaches were selected to be representative of the majority of studies listed in the review. These segmentation strategies, which will be compared in the next section, are defined as follows:

  I. The outline of the whole tumor was drawn on the axial slice containing the largest tumor section (hereafter 'Whole Tumor').
 II. The outline of the whole tumor was defined as in [I], but drawn 2 mm within the outer edge to avoid partial volume effects (hereafter 'Inside').
III. The outline of the whole tumor was defined as in [I], excluding any necrotic, cystic, or hemorrhagic areas (hereafter 'Solid').
IV. The outline of the whole tumor was drawn slightly within the outer edge to avoid partial volume effects excluding any necrotic, cystic, or hemorrhagic areas (hereafter 'Inside Solid').
 V. A single circular ROI was drawn on the axial slice containing the largest tumor section, with the largest possible radius that does not exceed the tumor edges (hereafter 'Circle').
VI. Three circular ROIs placed in the most diffusion-restricted areas of the tumor were drawn on the axial slice containing the largest tumor section. The ROIs were drawn such as to maximize the total area within the diffusion-restricted component of the tumor but not exceed into the less restricted areas (hereafter 'Max DWI circles').

An example of these strategies is given in Fig. 2.

### Segmentation analysis

Figure 3 shows two example slices of the ADC and T1 post-contrast images for the considered patients.

**Table 1** The selected studies included patients with either rhabdomyosarcoma (RMS), osteosarcoma (OS), uterine sarcoma (US), chondrosarcoma (CS), leiomyosarcoma (LMS), pulmonary artery sarcoma (PAS), hepatic angiosarcoma (HA), endometrial stromal sarcoma (ESS), or multiple (soft tissue) sarcomas. Non-sarcoma patients not shown. The studies performed segmentation for either response assessment (RA), differentiation (diff), or other purposes. Studies marked with an asterisk (*) included multiple segmentation strategies

| First Author | Year | Sarcoma type | Patients | Reason | Volume | Process | Method | Image modality | References |
|---|---|---|---|---|---|---|---|---|---|
| Abdel Razek | 2013 | Multiple | 17 | Diff | 2D | Manual | Outline | Diffusion | [22] |
| Aktas | 2021 | Multiple | 42 | RA | Unclear | Manual | Unclear | Structural | [23] |
| Albalawi | 2019 | RMS | 26 | Other | 2D | Manual | Unclear | Diffusion | [24] |
| Alsharief | 2019 | Multiple | 21 | Diff | 2D | Manual | Circular ROI | Diffusion | [25] |
| Ashikyan | 2021 | Multiple | 15 | other | Unclear | Manual | Outline | Diffusion | [26] |
| Asmar | 2020 | Multiple | 15 | RA | 2D | Manual | Outline | Structural | [27] |
| Baidya Kayal | 2019 | OS | 40 | RA | 3D | Manual | Outline | Diffusion | [28] |
| Bajpai | 2009 | OS | 31 | Other | Unclear | Manual | Outline | Diffusion | [29] |
| Bajpai | 2011 | OS | 31 | RA | MS | Manual | Unclear | Diffusion | [30] |
| Banerjee | 2018 | RMS | 21 | Diff | 3D | Semi-Automated | Outline | Diffusion | [31] |
| Baunin | 2012 | OS | 15 | Diff | 2D | Manual | Unclear | Diffusion | [32] |
| Bi | 2018 | US | 60 | Diff | MS | Manual | Circular ROI | Diffusion | [33] |
| Bi | 2020 | US | 71 | Diff | 2D | Manual | Circular ROI | Diffusion | [34] |
| Bologna | 2017 | Multiple | 18 | Other | 3D | Manual | Outline | Diffusion | [35] |
| Bruegel | 2013 | HE | 7 | Other | 2D | Manual | Circular ROI | Diffusion | [36] |
| Byun | 2013 | OS | 28 | RA | 2D | Manual | Outline | Diffusion | [37] |
| Chhabra | 2019 | Multiple | 43 | Other | 2D | Manual | Circular ROI | Diffusion | [38] |
| Chodyla | 2021 | Multiple | 37 | diff | 3D | Manual | Outline | Diffusion | [39] |
| Chodyla | 2021 | Multiple | 52 | RA | 3D | Manual | Outline | Diffusion | [40] |
| Corino | 2018 | Multiple | 19 | Diff | 3D | Manual | Outline | Diffusion | [41] |
| Degnan | 2018 | Multiple | 18 | RA | 2D | Manual | Outline | Diffusion | [42] |
| Del Grande | 2014 | Multiple | 37 | Other | Unclear | Manual | Unclear | Diffusion | [43] |
| Dudeck | 2008 | Multiple | 23 | RA | MS | Manual | Circular ROI | Diffusion | [44] |
| Einarsdóttir | 2004 | Multiple | 13 | Other | 2D | Manual | Outline | Diffusion | [45] |
| Gao | 2017 | RMS | 6 | RA | Unclear | Manual | Unclear | Diffusion | [46] |
| Gao | 2021 | Multiple | 30 | RA | Unclear | Manual | Outline | Diffusion | [47] |
| Gerges | 2018 | LMS | 17 | Diff | 3D | Manual | Outline | Diffusion | [48] |
| Habre | 2021 | OS | 26 | diff | 2D | Manual | Outline | Structural | [49] |
| Hao | 2021 | OS | 34 | RA | Unclear | Manual | Outline | Diffusion | [50] |
| Hélage | 2021 | US | 50 | diff | Unclear | Manual | Circular ROI | Diffusion | [51] |
| Hong | 2020 | Multiple | 12 | diff | 3D | Manual | Outline | Diffusion | [52] |
| Huang | 2019 | US | 20 | Diff | 2D | Manual | Outline | Unclear | [53] |
| Ioannidis | 2019 | Multiple | 22 | Other | 3D | Manual | Circular ROI | Diffusion | [54] |
| Kralik | 2018 | RMS | 12 | Diff | 2D | Manual | Outline | Diffusion | [55] |
| Lee | 2020 | Multiple | 36 | Other | 2D | Manual | Outline | Structural | [56] |
| Lee* | 2020 | OS | 35 | RA | Multiple | Manual | Multiple | Diffusion | [57] |
| Li | 2017 | LMS | 16 | Diff | MS | Manual | Circular ROI | Diffusion | [58] |
| Li | 2017 | ESS | 15 | Other | MS | Manual | Circular ROI | Diffusion | [59] |
| Li | 2021 | Multiple | 40 | other | 2D | Manual | Outline | Diffusion | [60] |
| Li | 2021 | Multiple | 34 | other | 2D | Manual | Outline | Diffusion | [61] |
| Liu | 2017 | PAS | 6 | Diff | 2D | Manual | Circular ROI | Diffusion | [62] |
| Liu | 2019 | OS | 29 | RA | 2D | Manual | Outline | Diffusion | [63] |
| Manikis | 2021 | Multiple | 28 | diff | 3D | Manual | Outline | Diffusion | [64] |
| Müller | 2016 | CS | 32 | Diff | 2D | Manual | Outline | Diffusion | [65] |
| Nakagawa | 2019 | US | 11 | Diff | 3D | Manual | Outline | Structural | [66] |
| Nakagawa | 2019 | US | 30 | Diff | 2D | Manual | Outline | Structural | [67] |

Chatziantoniou *et al. Insights into Imaging*      (2023) 14:19

Page 6 of 15

**Table 1** (continued)

| First Author | Year | Sarcoma type | Patients | Reason | Volume | Process | Method | Image modality | References |
|---|---|---|---|---|---|---|---|---|---|
| Oka | 2010 | OS | 22 | RA | 2D | Manual | Circular ROI | Diffusion | [68] |
| Orsatti | 2021 | Multiple | 13 | RA | 3D | Manual | Outline | Diffusion | [69] |
| Oztürk | 2021 | Multiple | 18 | other | Unclear | Manual | Circular ROI | Diffusion | [70] |
| Parlak | 2021 | Multiple | 35 | diff | Unclear | Manual | Outline | Diffusion | [71] |
| Pourmehdi Lahiji | 2019 | RMS | 21 | RA | 2D | Manual | Outline | Diffusion | [9] |
| Rio | 2019 | LMS | 20 | Diff | 2D | Manual | Circular ROI | Diffusion | [72] |
| Sagiyama | 2017 | Multiple | 22 | Diff | 3D | Manual | Outline | Structural | [73] |
| Saleh | 2020 | Multiple | 104 | RA | 2D | Manual | Circular ROI | Diffusion | [74] |
| Schnapauff | 2009 | Multiple | 30 | Other | Unclear | Manual | Circular ROI | Diffusion | [75] |
| Singer* | 2016 | Multiple | 17 | Other | Multiple | Multiple | Multiple | Diffusion | [21] |
| Soldatos | 2016 | Multiple | 23 | RA | Unclear | Manual | Unclear | Diffusion | [76] |
| Sumi | 2015 | US | 25 | Diff | Unclear | Manual | Outline | Diffusion | [77] |
| Teo | 2021 | OS | 15 | RA | 3D | Manual | Outline | Structural | [78] |
| Tian | 2021 | US | 14 | diff | Unclear | Manual | Unclear | Diffusion | [79] |
| Tong | 2019 | LMS | 10 | Other | Unclear | Manual | Outline | Diffusion | [80] |
| Uhl | 2006 | OS | 8 | RA | 2D | Manual | Outline | Diffusion | [81] |
| Uhl | 2006 | OS | 8 | RA | 2D | Manual | Outline | Diffusion | [82] |
| Valdes-Devesa | 2019 | Multiple | 10 | Diff | Unclear | Manual | Outline | Diffusion | [83] |
| Vossen | 2008 | LMS | 10 | RA | 2D | Manual | Unclear | Diffusion | [84] |
| Wang | 2013 | OS | 35 | RA | Unclear | Manual | Outline | Diffusion | [85] |
| Wang | 2017 | OS | 12 | RA | 2D | Manual | Circular ROI | Diffusion | [86] |
| Welzel | 2018 | CS | 35 | Diff | Unclear | Manual | Outline | Diffusion | [87] |
| Wu | 2018 | Multiple | 22 | Diff | MS | Manual | Outline | Diffusion | [88] |
| Xie | 2019 | US | 29 | Diff | 3D | Manual | Outline | Diffusion | [89] |
| Xing | 2018 | Multiple | 7 | Diff | Unclear | Manual | Outline | Structural | [90] |
| Yakushiji | 2009 | Multiple | 40 | Other | Unclear | Manual | Outline | Diffusion | [91] |
| Yang | 2016 | Multiple | 3 | RA | 2D | Manual | Outline | Diffusion | [92] |
| Yu | 2021 | Multiple | 6 | other | Unclear | Manual | Unclear | Unclear | [93] |
| Zeitoun | 2018 | OS | 31 | Diff | 2D | Manual | Circular ROI | Diffusion | [94] |
| Zhang | 2022 | Multiple | 41 | other | 2D | Manual | Outline | Diffusion | [95] |

The percentage change between the mean ADC of all included voxels was calculated pairwise for all segmentation strategies. This is shown in Table 3. Excluding the edge yields a minor difference. Excluding necrotic, cystic, or hemorrhagic components results in a decrease in the mean ADC of around 6%. Placing a circular ROI instead of an outline yields a minor difference. Only measuring the most diffusion-restricted areas results in a decrease in the mean ADC of around 20%. The table furthermore shows whether the ADC distributions differ significantly as determined by the two-sample Kolmogorov–Smirnov test. Apart from the combinations of 'Whole Tumor'—'Inside' and 'Solid'—'Inside Solid', all pairwise comparisons result in statistical differences.

Figure 4 shows the ADC distribution per patient for each of the six segmentation strategies. In patients where the tumor has a large necrotic component (1 and 4), there is a visible difference between strategies that exclude this component and those that do not. Not excluding the necrotic areas results in a small additional peak in the histogram.

Figure 5 shows the ADC distributions obtained by applying each segmentation strategy on two nearby slices for each patient. The distributions change visibly for patients 3–5 for each strategy. For patients 1 and 2, this difference is less clear from the shape of the distribution. When tested with the Kolmogorov–Smirnov test, there is a significant difference between the ADC distributions measured this way for all patients and all segmentation strategies.

The percentage change of the mean ADC of each tumor between two nearby slices averaged for all methods was small for patients 1–2 (4.55% and 5.42%), moderate for patients 4–5 (15.33% and 11.23%), and very large for patient 3 (96.0%). The values for all methods and patients are shown in Table 4.

**Table 2** There is a high degree of variation in certain aspects of the segmentation strategy, such as the method, volume, and area. Other aspects, like the process and image modality, are more homogeneous

| Property | Option | N |
|---|---|---|
| Method | Outline | 49 |
| | Circular ROI | 22 |
| | Unclear | 10 |
| Volume | 2D | 36 |
| | Multislice | 7 |
| | 3D | 17 |
| | Unclear | 21 |
| Process | Manual | 79 |
| | Semi-Automated | 2 |
| Image Modality | Structural | 9 |
| | Diffusion | 70 |
| | Unclear | 2 |
| Area | Excludes edge | 6 |
| | Excludes other | 15 |
| | Specific area | 22 |
| | Whole tumor | 39 |
| | Multiple ROIs | 7 |
| | Unclear | 6 |

## Discussion

In this study, we investigate the effect of segmentation strategies on the computation of ADC values in patients with sarcoma. With a literature review, we show the existence of a large variety of methods that are applied in the field. Furthermore, we demonstrate with data from a small sample of pediatric rhabdomyosarcoma patients that applying different methods can significantly affect the measured ADC value.

### Literature review

Most prior investigations to date on the variability due to segmentation methods have focused on the effect of raters or algorithms [16, 17], even when extending the search beyond sarcomas. One notable study by Schurink and colleagues looked at both interrater differences as well as single- and multislice segmentations [18] and found that the segmentation volume affects most radiomics much more than the experience of the rater.

Our literature review shows that there is a consensus between most studies for performing the segmentation on DWI and not on structural images, as well as a clear preference for manual segmentation as opposed to semi-automated methods. Conversely, no consensus or even established strategy could be determined regarding
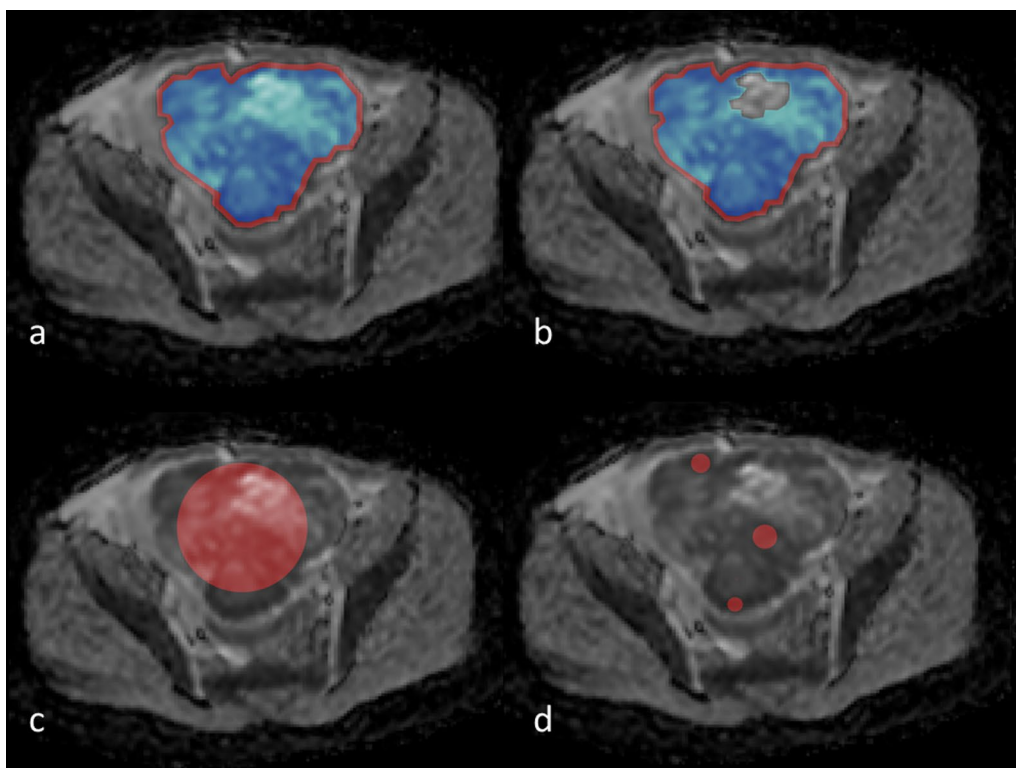


**Fig. 2** Illustrative example of diffusion-weighted image with regions of interest (ROIs) of six commonly used segmentation areas highlighted. **a** 'Inside' strategy, blue area. 'Whole tumor' strategy, red + blue area. **b** 'Inside solid' strategy, blue area. 'Solid' strategy, red + blue area. **c** 'Circle' strategy. **d** 'Max DWI circles' strategy
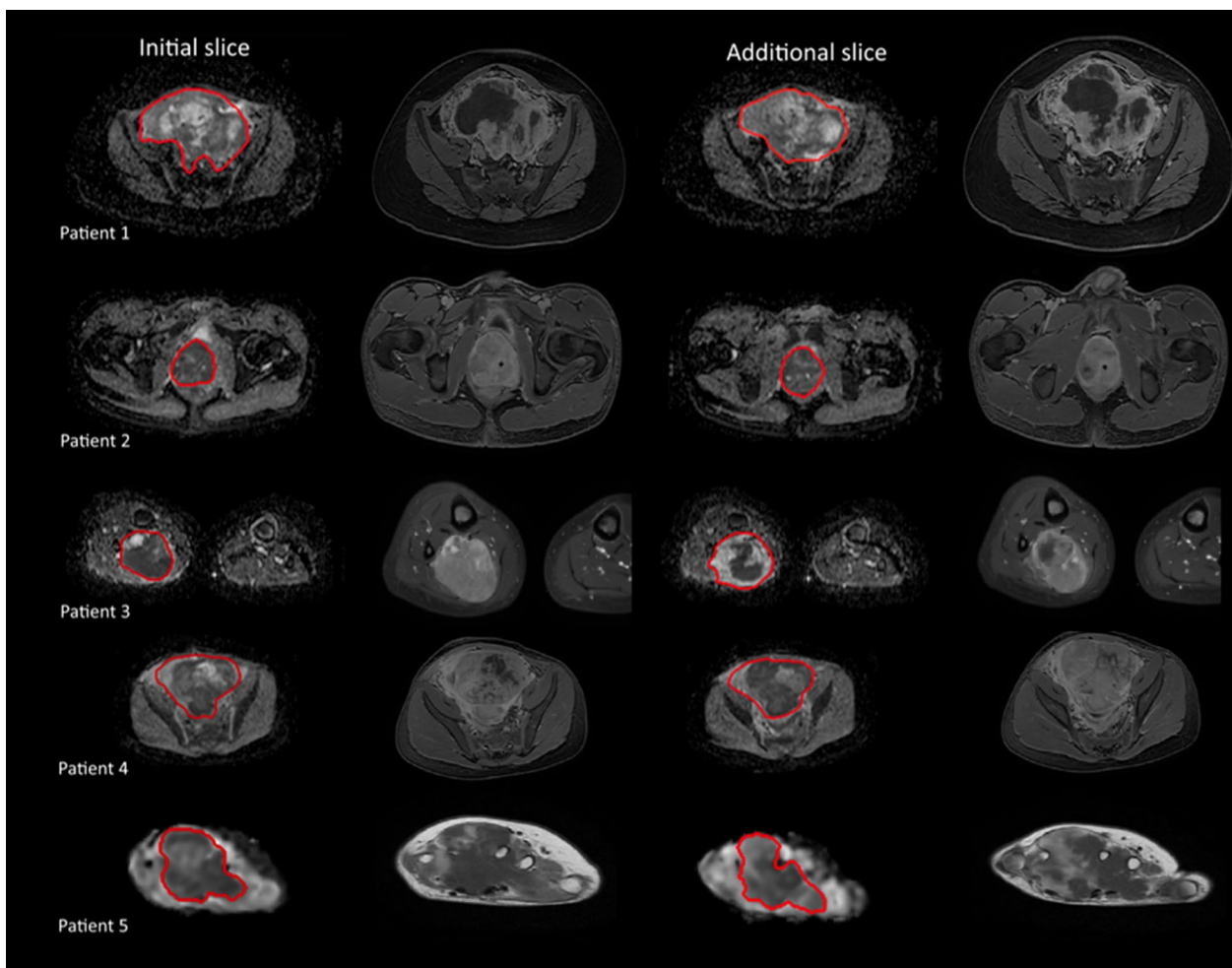
Chatziantoniou *et al. Insights into Imaging* (2023) 14:19

Page 8 of 15



**Fig. 3** Apparent diffusion coefficient (ADC) maps and T1 post-contrast images for both the initial slice (columns 1 and 2) and the additional slice (columns 3 and 4) where segmentations have been made. The ADC maps include the outline of segmentation strategy 1 as described in Results

**Table 3** Percent difference of the mean apparent diffusion coefficient (ADC) averaged over all patients between every pair of strategies described in Methods

| Method | Whole tumor (%) | Inside (%) | Solid (%) | Inside solid (%) | Circle (%) | Max DWI circles (%) |
|---|---|---|---|---|---|---|
| Whole tumor | | 0.50 | **− 5.58** | **− 5.82** | **0.73** | **− 21.66** |
| Inside | − 0.50 | | **− 6.05** | **− 6.30** | **0.23** | **− 22.05** |
| Solid | **5.91** | **6.44** | | − 0.26 | **6.68** | **− 17.03** |
| Inside solid | **6.18** | **6.72** | 0.26 | | **6.96** | **− 16.81** |
| Circle | **− 0.73** | **− 0.23** | **− 6.27** | **− 6.51** | | **− 22.23** |
| Max DWI circles | **27.65** | **28.29** | **20.53** | **20.21** | **28.58** | |

Bold numbers indicate significantly different distributions as determined by the two-sample Kolmogorov–Smirnov test. Excluding the edge from an ROI yields no significant differences in the distribution. All other methods do yield different distributions

the segmentation method (outline or circular), the area inclusion, and the segmentation volume.

Examining the reason for such a diversity of strategies is difficult given that segmentation approaches are often presented without any supporting evidence or
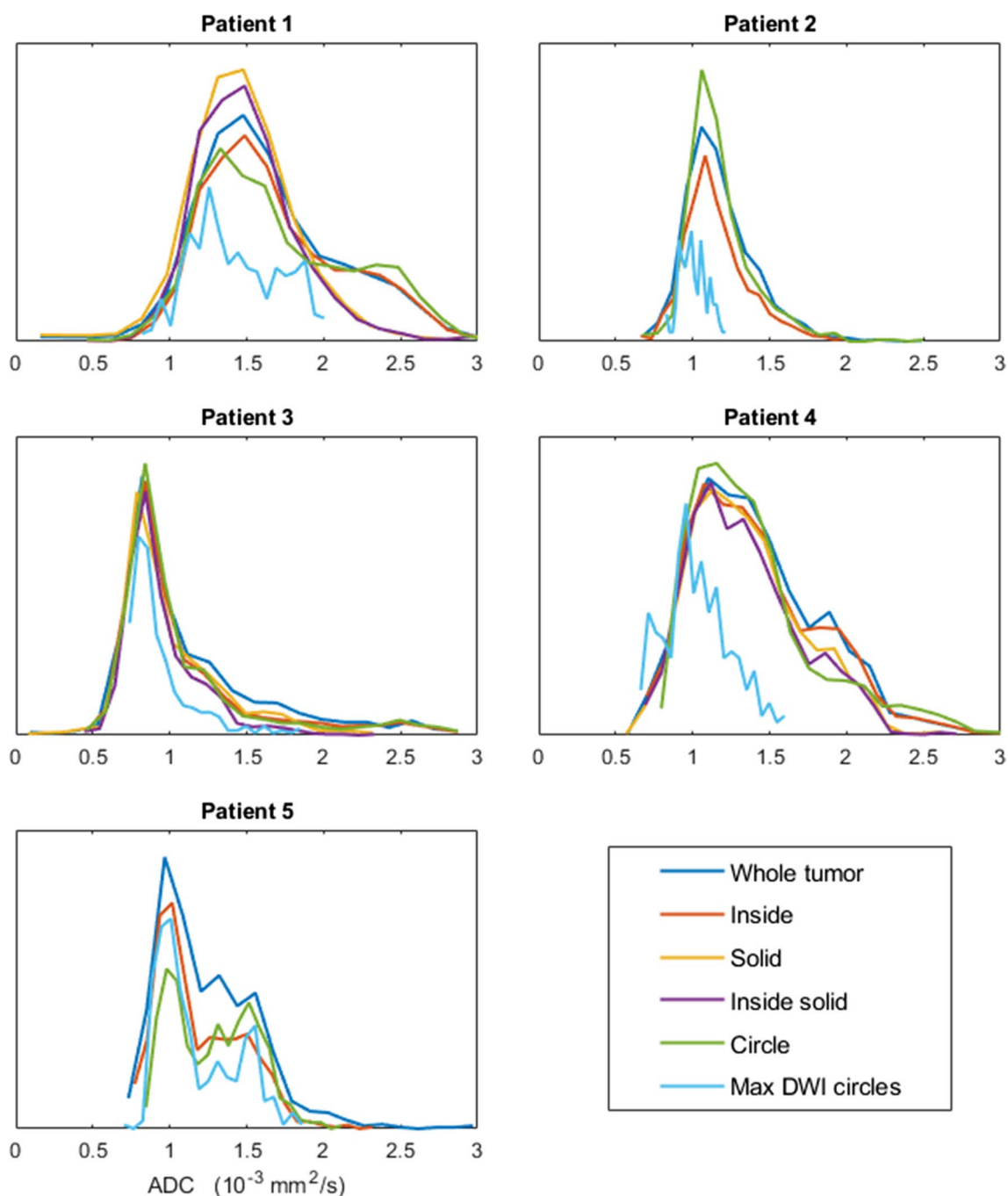
**Fig. 4** Normalized histograms of the apparent diffusion coefficient (ADC) of different regions of interest (ROIs) acquired with the strategies described in Methods. Varying segmentation methods can yield different distributions of the measured diffusion. Including necrotic, cystic, or hemorrhagic regions can result in non-Gaussian distributions. Patients 2 and 5 did not show any necrotic, cystic, or hemorrhagic tumor components and as such, specific ROIs that exclude these have not been drawn

rationale for their choice. We find that only eight out of the 76 included studies refer to previous literature to justify some aspects of their methods. It therefore remains unclear whether any particular strategy was chosen based on its effectiveness or its ease of implementation.

Furthermore, many specific aspects needed for reproducibility are sometimes either not reported well or not at all. Out of all included studies, 27 did not report all aspects of the segmentation applied. A further 20 were excluded from the review altogether for not reporting any details.
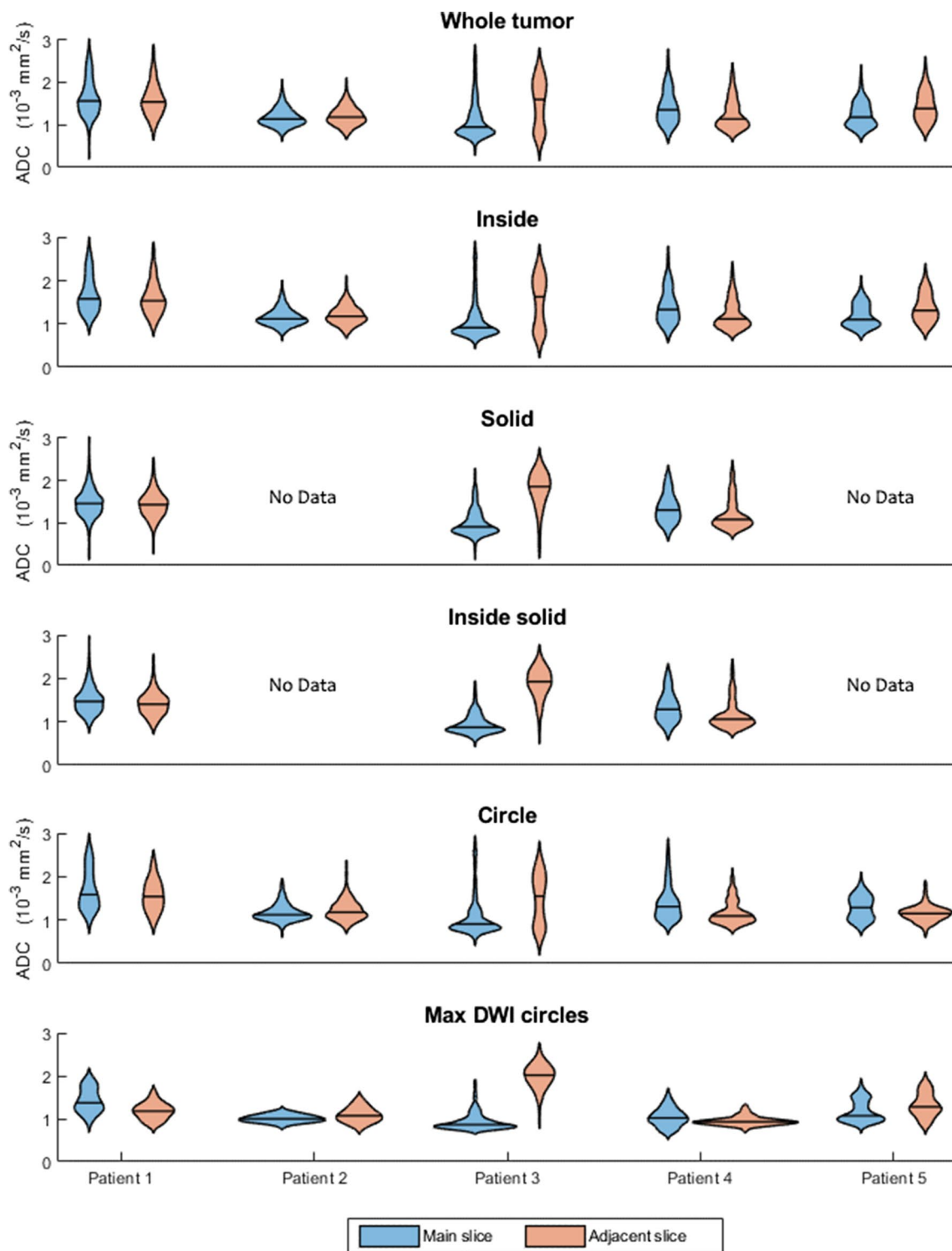
**Fig. 5** Violin plots of the apparent diffusion coefficient (ADC) estimated on two slices spaced two slices apart from each other. The estimations were derived from five patients with the regions of interest (ROIs) as defined by the six different segmentation strategies. Patients 2 and 5 did not show any necrotic, cystic, or hemorrhagic tumor components and as such, specific ROI that excludes these have not been drawn

Chatziantoniou *et al. Insights into Imaging*    (2023) 14:19

Page 11 of 15

**Table 4** Percentage difference of mean ADC when measuring with the same strategy on a slice two steps down in the caudal direction. The measured mean ADC can drastically vary between nearby slices if the tumor is heterogeneous. No measurements were done with the solid strategy on patients 2 and 5, as these did not have any necrotic, cystic, or hemorrhagic components. All methods yield significantly different distributions as determined by the two-sample Kolmogorov–Smirnov test

| Method | Patient (%) | | | | |
|---|---|---|---|---|---|
| | 1 | 2 | 3 | 4 | 5 |
| Whole tumor | 3.43 | 3.03 | 33.66 | 11.99 | 15.37 |
| Inside | 5.26 | 4.86 | 38.80 | 13.81 | 15.43 |
| Solid | 2.86 | | 77.16 | 10.99 | |
| Inside solid | 5.59 | | 98.58 | 13.31 | |
| Circle | 7.62 | 5.32 | 37.37 | 16.11 | 10.48 |
| Max DWI circles | 17.45 | 8.20 | 111.96 | 8.36 | 12.40 |
| Mean | 7.03 | 5.35 | 66.26 | 12.43 | 13.42 |

This large degree of variation highlights a need for a standard for reporting details on tumor segmentation, in analogy to other established radiological practices [19].

Altogether, when looking at segmentation strategies, we find a lack of reported details, a large variability of literature, and a lack of evidence-based strategies. This suggests that segmentation might often be an afterthought in study design.

### Segmentation analysis

When comparing different segmentation strategies for estimating ADC values from pediatric rhabdomyosarcoma cases, we find that the choice of segmentation area can affect the measured ADC. Most notably, excluding necrotic, cystic, and hemorrhagic areas results in a decrease of 5.6% in the mean ADC. It furthermore results in an ADC distribution that is more Gaussian than when including such regions. Next, measuring only the most diffusion-restricted parts of the tumor results in a decrease of 21.6%. The resulting segmentation contains too few voxels to create a useful ADC distribution. Additionally, drawing a circular ROI instead of an outline results in a small, but still significant, difference in ADC ($< 1\%$). Finally, excluding the most peripheral areas of the tumor does not result in any significant differences to the mean ADC or ADC distribution.

Varying the slice on which segmentations are made has a much larger effect, especially for heterogeneous tumors. When looking at all patients and all strategies, the mean ADC averaged a 26.5% difference when measured on a nearby slice. These results are in line with results described by Guo and colleagues [20], who compared 2D and 3D ROIs on 56 patients with breast phyllodes tumors. They found that single-slice segmentations generally resulted in a higher ADC. Similarly, Singer and colleagues [21] compared four different segmentation strategies on data of 22 patients with soft tissue lesions. They showed that whole-tumor segmentations resulted in lower ADC values compared to single-slice and multi-slice segmentations. Such a large difference in mean ADC measured across nearby slices is striking when considering that more than half of the included studies are using single-slice segmentations. As this method can produce strongly varying results—especially in heterogeneous tumors—care should be taken when using it and preference should be given to methods annotating multiple slices, where possible.

For pediatric rhabdomyosarcoma specifically, it would be useful to further investigate the effect of different segmentation strategies. As the disease is rare, any sufficiently powerful study requires a multicentric design. Since such a design typically already entangles variability in terms of acquisition hardware and protocols, better understanding the additional variance introduced by different segmentation methods could help maximizing statistical power in this field.

### Considerations

Rhabdomyosarcoma is the primary focus of this review. As an insufficient number of studies in this field described the segmentation approach with sufficient detail, the search was expanded to include other types of soft tissue sarcoma, including ones only arising in adults. As these other types of sarcomas might exhibit different radiological manifestations, segmentation strategies used in their study might differ from those used in rhabdomyosarcoma.

Another limitation of our study is that only five patients were included in our segmentation analysis. This small number might bias our results toward individual properties and may not represent the 'average' patient with rhabdomyosarcoma. However, even with such limited sample size we are able to demonstrate that certain aspects of the segmentation strategy can affect ADC measurements, showing proof of concept of the importance to design and report tumor segmentation strategies. Finally, we only assessed the impact of the measurement site and method on the initial measurement and not on the impact on tumor response assessment.

### Conclusion

There is a large variation in segmentation strategies for sarcomas. This variation is difficult to characterize, as many articles do not justify why a strategy is chosen. Details of the segmentation method are furthermore

Chatziantoniou *et al. Insights into Imaging*     (2023) 14:19

Page 12 of 15

often not well reported or not reported at all. When comparing strategies on our own data, we find that ADC estimates derived from a single slice depend highly on their location within the tumor. For this reason, using multi-slice or full-volume segmentations is preferred.

We call upon researchers to include clear imaging and reporting guidelines in protocols of prospective multi-center studies. It is our advice to keep in mind how the segmentation strategy might affect any computations made and to report all of the important details for making segmentations reproducible.

## Abbreviations
ADC        Apparent diffusion coefficient
DWI        Diffusion-weighted imaging
MRI        Magnetic resonance imaging
ROI        Region of interest

## Supplementary Information
The online version contains supplementary material available at https://doi.org/10.1186/s13244-022-01351-z.

> **Additional file 1:** Search terms used in PubMed literature search on 24-03-2022.

## Author contributions
AL, RS, and AdL contributed to conception and designs; CC, AdL, and RS were involved in methodology; RvE, StH, and RvR contributed to data acquisition; CC was involved in data analysis and drafted the article; and all authors substantially revised the article. All authors have read and approved the final version and have agreed both to be personally accountable for the author's own contribution and to ensure that questions related to the accuracy or integrity of any part of the work, even ones in which the authors was not personally involved, are appropriately investigated, resolved, and the resolution documented in the studies. All authors read and approved the final manuscript.

## Availability of data and materials
The datasets analyzed during this study are available from the corresponding author on reasonable request.

## Declarations

### Ethical approval and consent to participate
The study was conducted in accordance with the Declaration of Helsinki and the GCP guideline. Written informed consent from patients and/or their parents or legal guardians was obtained.

### Consent for publication
Not applicable.

### Consent for publication
Not applicable.

### Competing interests
The authors declare that they have no competing interest.

## Author details
[1]Image Sciences Institute, UMC Utrecht, Utrecht, The Netherlands. [2]Princess Máxima Center for Pediatric Oncology, Utrecht, The Netherlands. [3]Department of Neurology, UMC Utrecht Brain Center, UMCUtrecht, Utrecht, The Netherlands. [4]Department of Radiology and Nuclear Medicine, Amsterdam UMC Location University of Amsterdam, Amsterdam, The Netherlands. [5]Department of Radiology and Nuclear Medicine, Wilhelmina Children's Hospital UMC Utrecht, Utrecht, The Netherlands.

## References
1. Schoot RA, McHugh K, van Rijn RR et al (2013) Response assessment in pediatric rhabdomyosarcoma: can response evaluation criteria in solid tumors replace three-dimensional volume assessments? Radiology 269:870–878. https://doi.org/10.1148/RADIOL.13122607
2. van Ewijk R, Vaarwerk B, Breunis WB (2021) The value of early tumor size response to chemotherapy in pediatric rhabdomyosarcoma. Cancers 13:510. https://doi.org/10.3390/CANCERS13030510
3. Suzuki C, Torkzad MR, Jacobsson H et al (2010) Interobserver and intraobserver variability in the response evaluation of cancer therapy according to RECIST and WHO-criteria. Acta Oncol 49:509–514. https://doi.org/10.3109/02841861003705794
4. Vaarwerk B, van der Lee JH, Breunis WB et al (2018) Prognostic relevance of early radiologic response to induction chemotherapy in pediatric rhabdomyosarcoma: a report from the International Society of Pediatric Oncology Malignant Mesenchymal Tumor 95 study. Cancer 124:1016–1024. https://doi.org/10.1002/CNCR.31157
5. Ermoian RP, Breneman J, Walterhouse DO et al (2017) 45 Gy is not sufficient radiotherapy dose for Group III orbital embryonal rhabdomyosarcoma after less than complete response to 12 weeks of ARST0331 chemotherapy: a report from the Soft Tissue Sarcoma Committee of the Children's Oncology Group. Pediatr Blood Cancer. https://doi.org/10.1002/PBC.26540
6. Rosenberg AR, Anderson JR, Lyden E et al (2014) Early response as assessed by anatomic imaging does not predict failure-free survival among patients with Group III rhabdomyosarcoma: a report from the Children's Oncology Group. Eur J Cancer 50:816–823. https://doi.org/10.1016/J.EJCA.2013.11.031
7. Burke M, Anderson JR, Kao SC et al (2007) Assessment of response to induction therapy and its influence on 5-year failure-free survival in group III rhabdomyosarcoma: the intergroup rhabdomyosarcoma study-IV experience - A report from the Soft Tissue Sarcoma Committee of the Children's Oncology Group. J Clin Oncol 25:4909–4913. https://doi.org/10.1200/JCO.2006.10.4257
8. Norman G, Fayter D, Lewis-Light K, McHugh K, Levine D, Phillips B (2014) (2014) Mind the gap: extent of use of diffusion-weighted MRI in children with rhabdomyosarcoma. Pediatr Radiol 455(45):778–781. https://doi.org/10.1007/S00247-014-3120-Z
9. Pourmehdi Lahiji A, Jackson T, Nejadnik H et al (2019) Association of tumor [18F]FDG activity and diffusion restriction with clinical outcomes of rhabdomyosarcomas. Mol Imaging Biol 21:591–598. https://doi.org/10.1007/s11307-018-1272-1
10. Galbán CJ, Hoff BA, Chenevert TL, Ross BD (2017) Diffusion MRI in early cancer therapeutic response assessment. NMR Biomed 30:e3458
11. Humphries PD, Sebire NJ, Siegel MJ, Olsen ØE (2007) Tumors in pediatric patients at diffusion-weighted MR imaging: apparent diffusion coefficient and tumor cellularity. Radiology 45:848–854. https://doi.org/10.1148/radiol.2452061535
12. Reichardt W, Juettner E, Uhl M, Elverfeldt DV, Kontny U (2009) Diffusion-weighted imaging as predictor of therapy response in an animal model of ewing sarcoma. Invest Radiol 44:298–303. https://doi.org/10.1097/RLI.0b013e31819dcc84
13. Raafat TA, Kaddah RO, Bokhary LM, Sayed HA, Awad AS (2021) The role of diffusion-weighted MRI in assessment of response to chemotherapy in osteosarcoma. Egypt J Radiol Nucl Med. https://doi.org/10.1186/s43055-020-00392-y

14. Ognjanovic S, Linabery AM, Charbonneau B, Ross JA (2009) Trends in childhood rhabdomyosarcoma incidence and survival in the United States, 1975–2005. Cancer 115:4218–4226. https://doi.org/10.1002/CNCR.24465

15. Bisogno G, Jenney M, Bergeron C et al (2018) Addition of dose-intensified doxorubicin to standard chemotherapy for rhabdomyosarcoma (EpSSG RMS 2005): a multicentre, open-label, randomised controlled, phase 3 trial. Lancet Oncol 19:1061–1071. https://doi.org/10.1016/S1470-2045(18)30337-1

16. Bossuyt PM, Reitsma JB, Bruns DE et al (2015) STARD 2015: an updated list of essential items for reporting diagnostic accuracy studies. Radiology 277:826–832. https://doi.org/10.1148/radiol.2015151516

17. Granzier RWY, Verbakel NMH, Ibrahim A et al (2020) MRI-based radiomics in breast cancer: feature robustness with respect to inter-observer segmentation variability. Sci Rep. https://doi.org/10.1038/S41598-020-70940-Z

18. Joskowicz L, Cohen D, Caplan N, Sosna J (2018) Automatic segmentation variability estimation with segmentation priors. Med Image Anal 50:54–64. https://doi.org/10.1016/J.MEDIA.2018.08.006

19. Schurink NW, van Kranen SR, Roberti S et al (2021) Sources of variation in multicenter rectal MRI data and their effect on radiomics feature reproducibility. Eur Radiol 1:1–11. https://doi.org/10.1007/S00330-021-08251-8/FIGURES/4

20. Guo Y, Tang WJ, Kong Q et al (2019) Can whole-tumor apparent diffusion coefficient histogram analysis be helpful to evaluate breast phyllode tumor grades? Eur J Radiol 114:25–31. https://doi.org/10.1016/J.EJRAD.2019.02.035

21. Singer AD, Pattany PM, Fayad LM, Tresley J, Subhawong TK (2016) Volumetric segmentation of ADC maps and utility of standard deviation as measure of tumor heterogeneity in soft tissue tumors. Clin Imaging 40:386–391. https://doi.org/10.1016/J.CLINIMAG.2015.11.017

22. Abdel Razek AAK, Nada N (2013) Role of diffusion-weighted MRI in differentiation of masticator space malignancy from infection. Dentomaxillofacial Radiol. https://doi.org/10.1259/dmfr.20120183

23. Aktas E, Arikan SM, Ardıç F et al (2021) The importance of diffusion apparent diffusion coefficient values in the evaluation of soft tissue sarcomas after treatment. Polish J Radiol 86:e291. https://doi.org/10.5114/PJR.2021.106413

24. Albalawi ED, Alkatan HM, Elkhamary SM, Safieh LA, Maktabi AMY (2019) Genetic profiling of rhabdomyosarcoma with clinicopathological and radiological correlation. Can J Ophthalmol 54:247–257. https://doi.org/10.1016/j.jcjo.2018.03.011

25. Alsharief AN, Martinez-Rios C, Hopyan S et al (2019) Usefulness of diffusion-weighted MRI in the initial assessment of osseous sarcomas in children and adolescents. Pediatr Radiol 49:1201–1208. https://doi.org/10.1007/s00247-019-04436-y

26. Ashikyan O, Bradshaw SB, Dettori NJ, Hwang H, Chhabra A (2021) Conventional and advanced MR imaging insights of synovial sarcoma. Clin Imaging 76:149–155. https://doi.org/10.1016/J.CLINIMAG.2021.02.010

27. Asmar K, Saade C, Salman R et al (2020) The value of diffusion weighted imaging and apparent diffusion coefficient in primary Osteogenic and Ewing sarcomas for the monitoring of response to treatment: Initial experience. Eur J Radiol 124:108855. https://doi.org/10.1016/J.EJRAD.2020.108855

28. Baidya Kayal E, Kandasamy D, Khare K, Bakhshi S, Sharma R, Mehndiratta A (2019) Intravoxel incoherent motion (IVIM) for response assessment in patients with osteosarcoma undergoing neoadjuvant chemotherapy. Eur J Radiol. https://doi.org/10.1016/j.ejrad.2019.08.004

29. Bajpai J, Gamanagatti S, Sharma MC et al (2009) Noninvasive imaging surrogate of angiogenesis in osteosarcoma. Pediatr Blood Cancer. https://doi.org/10.1002/pbc.22328

30. Bajpai J, Gamnagatti S, Kumar R et al (2011) Role of MRI in osteosarcoma for evaluation and prediction of chemotherapy response: correlation with histological necrosis. Pediatr Radiol 41:441–450. https://doi.org/10.1007/s00247-010-1876-3

31. Banerjee I, Crawley A, Bhethanabotla M, Daldrup-Link HE, Rubin DL (2018) Transfer learning on fused multiparametric MR images for classifying histopathological subtypes of rhabdomyosarcoma. Comput Med Imaging Graph 65:167–175. https://doi.org/10.1016/j.compmedimag.2017.05.002

32. Baunin C, Schmidt G, Baumstarck K et al (2012) Value of diffusion-weighted images in differentiating mid-course responders to

chemotherapy for osteosarcoma compared to the histological response: Preliminary results. Skeletal Radiol 41:1141–1149. https://doi.org/10.1007/s00256-012-1360-2

33. Bi Q, Xiao Z, Lv F, Liu Y, Zou C, Shen Y (2018) Utility of clinical parameters and multiparametric MRI as predictive factors for differentiating uterine sarcoma from atypical leiomyoma. Acad Radiol 25:993–1002. https://doi.org/10.1016/j.acra.2018.01.002

34. Bi Q, Wu K, Lv F, Xiao Z, Xiong Y, Shen Y (2020) The value of clinical parameters combined with magnetic resonance imaging (MRI) features for preoperatively distinguishing different subtypes of uterine sarcomas An observational study (STROBE compliant). Medicine (Baltimore). https://doi.org/10.1097/MD.0000000000019787

35. Bologna M, Montin E, Corino VDA, Mainardi LT (2017) Stability assessment of first order statistics features computed on ADC maps in soft-tissue sarcoma. In: Proceedings of the annual international conference of the IEEE engineering in medicine and biology society, EMBS. Institute of electrical and electronics engineers Inc., pp 612–615

36. Bruegel M, Muenzel D, Waldt S, Specht K, Rummeny EJ (2013) Hepatic angiosarcoma: Cross-sectional imaging findings in seven patients with emphasis on dynamic contrast-enhanced and diffusion-weighted MRI. Abdom Imaging 38:745–754. https://doi.org/10.1007/s00261-012-9967-2

37. Byun BH, Kong CB, Lim I et al (2013) Combination of 18F-FDG PET/CT and diffusion-weighted mr imaging as a predictor of histologic response to neoadjuvant chemotherapy: preliminary results in osteosarcoma. J Nucl Med 54:1053–1059. https://doi.org/10.2967/jnumed.112.115964

38. Chhabra A, Ashikyan O, Slepicka C et al (2019) Conventional MR and diffusion-weighted imaging of musculoskeletal soft tissue malignancy: correlation with histologic grading. Eur Radiol 29:4485–4494. https://doi.org/10.1007/s00330-018-5845-9

39. Chodyla M, Demircioglu A, Schaarschmidt BM et al (2021) Evaluation of 18F-FDG PET and DWI datasets for predicting therapy response of soft-tissue sarcomas under neoadjuvant isolated limb perfusion. J Nucl Med 62:348–353. https://doi.org/10.2967/JNUMED.120.248260

40. Chodyla M, Demircioglu A, Schaarschmidt BM et al (2021) Evaluation of the predictive potential of 18F-FDG PET and DWI data sets for relevant prognostic parameters of primary soft-tissue sarcomas. Cancers 13:2753. https://doi.org/10.3390/CANCERS13112753

41. Corino VDA, Montin E, Messina A et al (2018) Radiomic analysis of soft tissues sarcomas can distinguish intermediate from high-grade lesions. J Magn Reson Imaging 47:829–840. https://doi.org/10.1002/jmri.25791

42. Degnan AJ, Chung CY, Shah AJ (2018) Quantitative diffusion-weighted magnetic resonance imaging assessment of chemotherapy treatment response of pediatric osteosarcoma and Ewing sarcoma malignant bone tumors. Clin Imaging 47:9–13. https://doi.org/10.1016/j.clinimag.2017.08.003

43. Del Grande F, Subhawong T, Weber K, Aro M, Mugera C, Fayad LM (2014) Detection of soft-tissue sarcoma recurrence: added value of functional MR imaging techniques at 3.0 T. Radiology 271:499–511. https://doi.org/10.1148/radiol.13130844

44. Dudeck O, Zeile M, Pink D et al (2008) Diffusion-weighted magnetic resonance imaging allows monitoring of anticancer treatment effects in patients with soft-tissue sarcomas. J Magn Reson Imaging 27:1109–1113. https://doi.org/10.1002/jmri.21358

45. Einarsdóttir H, Karlsson M, Wejde J, Bauer HCF (2004) Diffusion-weighted MRI of soft tissue tumours. Eur Radiol 14:959–963. https://doi.org/10.1007/s00330-004-2237-0

46. Gao Y, Han F, Zhou Z et al (2017) Distortion-free diffusion MRI using an MRI-guided Tri-Cobalt 60 radiotherapy system: Sequence verification and preliminary clinical experience. Med Phys 44:5357–5366. https://doi.org/10.1002/mp.12465

47. Gao Y, Ghodrati V, Kalbasi A et al (2021) Prediction of soft tissue sarcoma response to radiotherapy using longitudinal diffusion MRI and a deep neural network with generative adversarial network-based data augmentation. Med Phys 48:3262–3372. https://doi.org/10.1002/MP.14897

48. Gerges L, Popiolek D, Rosenkrantz AB (2018) Explorative investigation of whole-lesion histogram MRI metrics for differentiating uterine leiomyomas and leiomyosarcomas. AJR Am J Roentgenol 210:1172–1177

49. Habre C, Dabadie A, Loundou AD et al (2021) Diffusion-weighted imaging in differentiating mid-course responders to chemotherapy

Chatziantoniou *et al. Insights into Imaging*        (2023) 14:19

Page 14 of 15

for long-bone osteosarcoma compared to the histologic response: an update. Pediatr Radiol 51:1714–1723. https://doi.org/10.1007/S00247-021-05037-4/TABLES/4

50. Hao Y, An R, Xue Y et al (2021) Prognostic value of tumoral and peritumoral magnetic resonance parameters in osteosarcoma patients for monitoring chemotherapy response. Eur Radiol 31:3518–3529. https://doi.org/10.1007/S00330-020-07338-Y/FIGURES/5

51. Hélage S, Vandeventer S, Buy JN et al (2021) Uterine sarcomas: are there MRI signs predictive of histopathological diagnosis? A 50-patient case series with pathological correlation. Sarcoma. https://doi.org/10.1155/2021/8880080

52. Hong JH, Jee WH, Jung CK, Jung JY, Shin SH, Chung YG (2019) Soft tissue sarcoma: adding diffusion-weighted imaging improves MR imaging evaluation of tumor margin infiltration. Eur Radiol 29:2589–2597

53. Huang YL, Ueng SH, Chen K et al (2019) Utility of diffusion-weighted and contrast-enhanced magnetic resonance imaging in diagnosing and differentiating between high- and low-grade uterine endometrial stromal sarcoma. Cancer Imaging. https://doi.org/10.1186/s40644-019-0247-z

54. Ioannidis GS, Nikiforaki K, Karantanas A (2019) Statistical and spatial correlation between diffusion and perfusion MR imaging parameters: a study on soft tissue sarcomas. Phys Medica 65:59–66. https://doi.org/10.1016/j.ejmp.2019.08.007

55. Kralik SF, Haider KM, Lobo RR, Supakul N, Calloni SF, Soares BP (2018) Orbital infantile hemangioma and rhabdomyosarcoma in children: differentiation using diffusion-weighted magnetic resonance imaging. J AAPOS 22:27–31. https://doi.org/10.1016/j.jaapos.2017.09.002

56. Lee SK, Jee W-H, Jung CK, Im SA, Chung N-G, Chung Y-G (2020) Prediction of poor responders to neoadjuvant chemotherapy in patients with osteosarcoma: additive value of diffusion-weighted MRI including volumetric analysis to standard MRI at 3T. PLoS One 15:0229983. https://doi.org/10.1371/JOURNAL.PONE.0229983

57. Lee JH, Yoon YC, Seo SW, Choi YL, Kim HS (2020) Soft tissue sarcoma: DWI and DCE-MRI parameters correlate with Ki-67 labeling index. Eur Radiol 30:914–924. https://doi.org/10.1007/s00330-019-06445-9

58. Li HM, Liu J, Qiang JW, Zhang H, Zhang GF, Ma F (2017) Diffusion-weighted imaging for differentiating uterine leiomyosarcoma from degenerated leiomyoma. J Comput Assist Tomogr 41:599–606. https://doi.org/10.1097/RCT.0000000000000565

59. Li HM, Liu J, Qiang JW, Gu WY, Zhang GF, Ma FH (2017) Endometrial stromal sarcoma of the uterus: Magnetic resonance imaging findings including apparent diffusion coefficient value and its correlation with Ki-67 expression. Int J Gynecol Cancer 27:1877–1887. https://doi.org/10.1097/IGC.0000000000001114

60. Li X, Yang L, Wang Q, Tao J, Pan Z, Wang S (2021) Soft tissue sarcomas: IVIM and DKI correlate with the expression of HIF-1α on direct comparison of MRI and pathological slices. Eur Radiol 31:4669–4679. https://doi.org/10.1007/S00330-020-07526-W/FIGURES/6

61. Li X, Liu Y, Tao J et al (2021) Value of intravoxel incoherent motion and diffusion kurtosis imaging in predicting peritumoural infiltration of soft-tissue sarcoma: a prospective study based on MRI–histopathology comparisons. Clin Radiol 76:532–539. https://doi.org/10.1016/J.CRAD.2021.02.014

62. Liu M, Luo C, Wang Y et al (2017) Multiparametric MRI in differentiating pulmonary artery sarcoma and pulmonary thromboembolism: a preliminary experience. Diagnost Interv Radiol 23:15–21. https://doi.org/10.5152/dir.2016.15584

63. Liu C, Xi Y, Li M et al (2019) Monitoring response to neoadjuvant chemotherapy of primary osteosarcoma using diffusion kurtosis magnetic resonance imaging: Initial findings. Korean J Radiol 20:801–811. https://doi.org/10.3348/kjr.2018.0453

64. Manikis GC, Nikiforaki K, Lagoudaki E et al (2021) Differentiating low from high-grade soft tissue sarcomas using post-processed imaging parameters derived from multiple DWI models. Eur J Radiol 138:109660. https://doi.org/10.1016/J.EJRAD.2021.109660

65. Müller U, Kubik-Huch RA, Ares C et al (2016) Is there a role for conventional MRI and MR diffusion-weighted imaging for distinction of skull base chordoma and chondrosarcoma? Acta Radiol 57:225–232. https://doi.org/10.1177/0284185115574156

66. Nakagawa M, Nakaura T, Namimoto T et al (2019) A multiparametric MRI-based machine learning to distinguish between uterine sarcoma and

benign leiomyoma: comparison with 18F-FDG PET/CT. Clin Radiol 74:167.e1-167.e7. https://doi.org/10.1016/j.crad.2018.10.010

67. Nakagawa M, Nakaura T, Namimoto T et al (2019) Machine learning to differentiate T2-weighted hyperintense uterine leiomyomas from uterine sarcomas by utilizing multiparametric magnetic resonance quantitative imaging features. Acad Radiol 26:1390–1399. https://doi.org/10.1016/j.acra.2018.11.014

68. Oka K, Yakushiji T, Sato H, Hirai T, Yamashita Y, Mizuta H (2010) The value of diffusion-weighted imaging for monitoring the chemotherapeutic response of osteosarcoma: a comparison between average apparent diffusion coefficient and minimum apparent diffusion coefficient. Skeletal Radiol 39:141–146. https://doi.org/10.1007/s00256-009-0830-7

69. Orsatti G, Zucchetta P, Varotto A et al (2021) Volumetric histograms-based analysis of apparent diffusion coefficients and standard uptake values for the assessment of pediatric sarcoma at staging: preliminary results of a PET/MRI study. Radiol Med 126:878–885. https://doi.org/10.1007/S11547-021-01340-0/FIGURES/4

70. Ozturk M, Polat AV, Tosun FC, Selcuk MB (2021) Does the SUVmax of FDG-PET/CT correlate with the ADC values of DWI in musculoskeletal malignancies? J Belgian Soc Radiol. https://doi.org/10.5334/JBSR.2378

71. Parlak Ş, Ergen FB, Yüksel GY et al (2021) Diffusion-weighted imaging for the differentiation of Ewing sarcoma from osteosarcoma. Skeletal Radiol 50:2023–2030. https://doi.org/10.1007/S00256-021-03741-8/TABLES/3

72. Rio G, Lima M, Gil R, Horta M, Cunha TM (2019) T2 hyperintense myometrial tumors: can MRI features differentiate leiomyomas from leiomyosarcomas? Abdom Radiol (NY) 44:3388–3397. https://doi.org/10.1007/s00261-019-02097-x

73. Sagiyama K, Watanabe Y, Kamei R et al (2017) Multiparametric voxel-based analyses of standardized uptake values and apparent diffusion coefficients of soft-tissue tumours with a positron emission tomography/magnetic resonance system: preliminary results. Eur Radiol 27:5024–5033. https://doi.org/10.1007/S00330-017-4912-y

74. Saleh MM, Abdelrahman TM, Madney Y, Mohamed G, Shokry AM, Moustafa AF (2020) Multiparametric MRI with diffusion-weighted imaging in predicting response to chemotherapy in cases of osteosarcoma and Ewing's sarcoma. Br J Radiol 93:20200257. https://doi.org/10.1259/bjr.20200257

75. Schnapauff D, Zeile M, Ben NM et al (2009) Diffusion-weighted echo-planar magnetic resonance imaging for the assessment of tumor cellularity in patients with soft-tissue sarcomas. J Magn Reson Imaging 29:1355–1359. https://doi.org/10.1002/jmri.21755

76. Soldatos T, Ahlawat S, Montgomery E, Chalian M, Jacobs MA, Fayad LM (2016) Multiparametric assessment of treatment response in high-grade soft-tissue sarcomas with anatomic and functional MR imaging sequences. Radiology 278:831–840. https://doi.org/10.1148/radiol.2015142463

77. Sumi A, Terasaki H, Sanada S et al (2015) Assessment of mr imaging as a tool to differentiate between the major histological types of uterine sarcomas. Magn Reson Med Sci 14:295–304. https://doi.org/10.2463/mrms.2014-0023

78. Teo KY, Daescu O, Cederberg K, Sengupta A, Leavey PJ (2022) Correlation of histopathology and multi-modal magnetic resonance imaging in childhood osteosarcoma: predicting tumor response to chemotherapy. PLoS One 17:e0259564. https://doi.org/10.1371/JOURNAL.PONE.0259564

79. Tian S, Niu M, Xie L, Song Q, Liu A (2021) Diffusion-tensor imaging for differentiating uterine sarcoma from degenerative uterine fibroids. Clin Radiol 76:313.e27-313.e32. https://doi.org/10.1016/J.CRAD.2020.11.115

80. Tong A, Kang SK, Huang C, Huang K, Slevin A, Hindman N (2019) MRI screening for uterine leiomyosarcoma. J Magn Reson Imaging 49:e282–e294. https://doi.org/10.1002/jmri.26630

81. Uhl M, Saueressig U, Van Buiren M et al (2006) Osteosarcoma: Preliminary results of in vivo assessment of tumor necrosis after chemotherapy with diffusion- and perfusion-weighted magnetic resonance imaging. Invest Radiol 41:618–623. https://doi.org/10.1097/01.rli.0000225398.17315.68

82. Uhl M, Saueressig U, Koehler G et al (2006) Evaluation of tumour necrosis during chemotherapy with diffusion-weighted MR imaging: preliminary results in osteosarcomas. Pediatr Radiol 36:1306–1311. https://doi.org/10.1007/s00247-006-0324-x

83. Valdes-Devesa V, del Mar Jimenez M, Sanz-Rosa D, Vaquero ME, Moreno EA, de la Cuesta Abbad RS (2019) Preoperative diagnosis of atypical pelvic leiomyoma and sarcoma: the potential role of diffusion-weighted

imaging. J Obstet Gynaecol 39:98–104. https://doi.org/10.1080/01443 615.2018.1466110

84. Vossen JA, Kamel IR, Buijs M et al (2008) Role of functional magnetic resonance imaging in assessing metastatic leiomyosarcoma response to chemoembolization. J Comput Assist Tomogr 32:347–352. https://doi. org/10.1097/RCT.0b013e318134ecd6

85. Wang CS, Du LJ, Si MJ et al (2013) Noninvasive assessment of response to neoadjuvant chemotherapy in osteosarcoma of long bones with diffusion-weighted imaging: an initial in vivo study. PLoS One. https://doi. org/10.1371/journal.pone.0072679

86. Wang J, Sun M, Liu D et al (2017) Correlation between apparent diffusion coefficient and histopathology subtypes of osteosarcoma after neoad-juvant chemotherapy. Acta Radiol 58:971–976. https://doi.org/10.1177/ 0284185116678276

87. Welzel T, Meyerhof E, Uhl M et al (2018) Diagnostic accuracy of DW MR imaging in the differentiation of chordomas and chondrosarcomas of the skull base: a 3.0-T MRI study of 105 cases. Eur J Radiol 105:119–124. https://doi.org/10.1016/j.ejrad.2018.05.026

88. Wu G, Liu X, Xiong Y, Ran J, Li X (2018) Intravoxel incoherent motion and diffusion kurtosis imaging for discriminating soft tissue sarcoma from vascular anomalies. Medicine (Baltimore). https://doi.org/10.1097/MD. 0000000000013641

89. Xie H, Zhang X, Ma S, Liu Y, Wang Y (2019) Preoperative differentiation of uterine sarcoma from leiomyoma: comparison of three models based on different segmentation volumes using radiomics. Mol Imaging Biol 21:1157–1164. https://doi.org/10.1007/s11307-019-01332-7

90. Xing S, Freeman CR, Jung S, Turcotte R, Levesque IR (2018) Probabilistic classification of tumour habitats in soft tissue sarcoma. NMR Biomed. https://doi.org/10.1002/nbm.4000

91. Yakushiji T, Oka K, Sato H et al (2009) Characterization of chondroblastic osteosarcoma: gadolinium-enhanced versus diffusion-weighted MR Imaging. J Magn Reson Imaging 29:895–900. https://doi.org/10.1002/ jmri.21703

92. Yang Y, Cao M, Sheng K et al (2016) Longitudinal diffusion MRI for treat-ment response assessment: preliminary experience using an MRI-guided tri-cobalt 60 radiotherapy system. Med Phys 43:1369–1373. https://doi. org/10.1118/1.4942381

93. Yu B, Huang C, Liu S et al (2021) Application of first-order feature analysis of DWI-ADC in rare malignant mesenchymal tumours of the maxillofacial region. BMC Oral Health 21:1–7. https://doi.org/10.1186/S12903-021-01835-2/FIGURES/2

94. Zeitoun R, Shokry AM, Ahmed Khaleel S, Mogahed SM (2018) Osteosar-coma subtypes: magnetic resonance and quantitative diffusion weighted imaging criteria. J Egypt Natl Canc Inst 30:39–44. https://doi.org/10. 1016/j.jnci.2018.01.006

95. Zhang K, Dai Y, Liu Y et al (2022) Soft tissue sarcoma: IVIM and DKI param-eters correlate with Ki-67 labeling index on direct comparison of MRI and histopathological slices. Eur Radiol 2022:1–10. https://doi.org/10.1007/ S00330-022-08646-1

## Publisher's Note

Springer Nature remains neutral with regard to jurisdictional claims in pub-lished maps and institutional affiliations.